2017

Impact of bedding plane and laminations on softening zone around the roadways – 3D numerical assessment

Mahdi Zoorabadi
SCT Operations, University of New South Wales, m.zoorabadi@sct.gs

Marzieh Rajabi
University of Wollongong

Publication Details
Mahdi Zoorabadi and Marzieh Rajabi, Impact of bedding plane and laminations on softening zone around the roadways – 3D numerical assessment, in Naj Aziz and Bob Kininmonth (eds.), Proceedings of the 17th Coal Operators' Conference, Mining Engineering, University of Wollongong, 8-10 February 2017, 32-40.

IMPACT OF BEDDING PLANE AND LAMINATIONS ON SOFTENING ZONE AROUND THE ROADWAYS – 3D NUMERICAL ASSESSMENT

Mahdi Zoorabadi[1] and Marzieh Rajabi[2]

ABSTRACT: When the distributed rock stress around the roadways exceeds the strength of the rock, the rock is failed and a softening zone is formed. Roof deformation developed in the roof and ribs of the roadways are highly controlled by the depth of softening zones. The rock failure process starts from a point ahead of the face and grows into the roof, floor and ribs by advancing roadway. The maximum stress that can be transferred through the failed rocks would be equal to its residual confined strength. Therefore, rock stress is moved above failed zone and will create new failure zone if it is higher than the confined strength of rock at that depth. This process continues until the confined strength of the rock becomes higher than stress components. Bedding and lamination planes play a big role into the failure pathway of rocks around roadways. The thickness of softening zone is significantly influenced by the shear and tensile strength of bedding planes and laminations. This paper presents a 3D numerical assessment of the bedding and lamination planes impacts to the forming and extension of the softening zones. It highlights the requirements for better characterisation of bedding and lamination planes for reliable simulation of roadways.

INTRODUCTION

Bedding planes and laminations are two common terminologies for sedimentary rocks. The stratification, which is the main sedimentary structure, is defined as layering of sediments throughout the sediment deposition. The stratification can be divided into two groups of bedding and lamination on the basis of the strata thickness. The lamination term is used when the strata thickness is less than 1 cm and it represents a sequence of fine layers. For the strata thicker than 1 cm, there are several sub-groups for description of bedding structure (Table 1). The bedding plane can be easily identified when the lithology of the adjacent beds is different (Figure 1). When the lithology of the adjacent beds is same (Figure 2), the bedding plane is hard to be recognised (Campbell, 1967).

Table 1: Bedding and lamination terminologies for sedimentary rocks (Campbell, 1967)

	Terminology	Strat Thickness [cm]
Bedding (Bed, Beds)	Very thick-bedded	> 100
	Thick-bedded	30 – 100
	Medium-bedded	10 – 30
	Thin-bedded	3 – 10
	Very thin-bedded	1 – 3
Lamination (Lamina, Laminate)	Laminated	0.3 – 1
	Thinly laminated	< 0.3

[1] *Senior Geotechnical Engineer, SCT Operations, Wollongong, Australia. Email m.zoorabadi@sct.gs Tel +61 2 4222 2777, Mob: +61 432 552 816, Adjunct Lecturer, School of Mining Engineering, UNSW Australia*
[2] *Mining Engineering Postgraduate Student, University of Wollongong, Australia.*

Figure 1: Bedding plane when lithology of the adjacent beds is different

Figure 2: Bedding plane when lithology of the adjacent beds is same

Shear strength of bedding planes and laminations can be determined by triaxial test or direct shear test. For direct shear test, the cores recovered from vertical or angled boreholes can be used. This test is more reliable for the shear strength of the partings. The following reasons limit the direct shear application for the tight bedding planes and laminations:

- Test setup: it is difficult to align the shearing direction correctly while casting the core into the upper and lower boxes.
- Loading boundary condition: providing pure shear loading condition is arguable because of developing tension stress on one side of the sample.

Considering the above limitations, the triaxial test is the best option to determine the shear strength of tight bedding planes. The bedding plane and laminations are acting as a weak plane within the sample. The Mohr-Coulomb failure criteria for a sample including a weak plane with an angle of β with the direction of maximum principal stress (σ_1) is as follow (Jaeger and Cook, 1979):

$$\sigma_1 - \sigma_3 = \frac{2(c+\sigma_3 tan\varphi)}{(1-tan\varphi cot\beta)sin2\beta}$$

where, σ_3 is minimum principal stress (confining stress), c is cohesion of intact rock, and φ represents the friction angle of the intact rock. For $\varphi < \beta < \pi/2$, the failure occurs along the weak plane. The graph of the maximum principal stress components against confining stresses represents the failure criteria for the weak plane.

The core samples for the tri-axial test on bedding plane are drilled at an angle to the bedding planes (Typically 30^o). This drilling angle provides samples with angle between the bedding plane and maximum principal stress of 60^o which guaranties the failure along the bedding plane. Figure 3 shows typical failure curves for the bedding planes obtained from direct shear and triaxial tests.

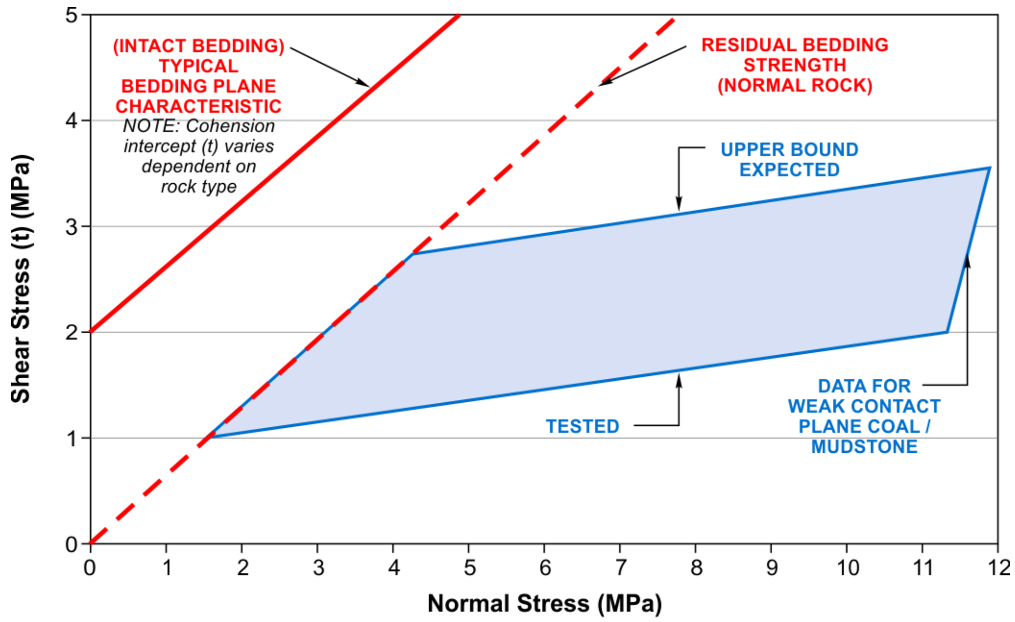

Figure 3: Typical strength characteristics of bedding planes and weak planes (SCT Operations 1995).

IMPACT OF BEDDING PLANES AND LAMINATIONS ON SOFTENING ZONE

In reality, roadway excavation removes the *in situ* confinement of the surrounding rocks. In considering the triaxial behaviour of rock, less confinement results in lower strength and more possibility for the redistributed stress to exceed the strength of rocks. When the new stress components exceed the strength of rocks, rocks fails in different modes. Apart from the failure of the intact rock, stress can exceeds the strength (tensile or shear strength) of the discontinuities such as bedding planes, lamination planes, and rock joints. Therefore combination and extension of all these failure modes create the softening zones around the roadway.

The historical field measurement showed that there is a relationship between the magnitude of roof deformation and the height of softening (Figure 4). The height of softening is defined by the height to which significant failure into the roof is occurring.

In this paper, 3D numerical simulation is implemented to study the impact of the bedding plane and the laminations to the extension of the softening zone around the roadway. FLAC3D (Itasca, 2013) was used for 3D simulation and SCT's rock failure simulation fish code (Gale, 1998) was extended to 3D and was applied for this analysis. In this numerical modelling, 1 m of rock is excavated as each excavation sequence and model is run to detect induced failure zone. This process is repeated to reach the desired excavation length of roadway. The length of modelled roadway should be enough to eliminate the boundary condition impacts. In failure simulation process, the strength of the material is determined on the basis of the confining pressure, friction angle and cohesion of the material, bedding and joints. The general strength characteristics of the rock materials in the intact and post failure range are presented in Figure 5. The model simulates rock fracture and stores the orientation of the fractures. Shear fracture, tension fracture of the rock, bedding plane shear and tension fracture of bedding is determined in the simulation. Failure modes obtained from this simulation are presented by different numbers (Table 2).

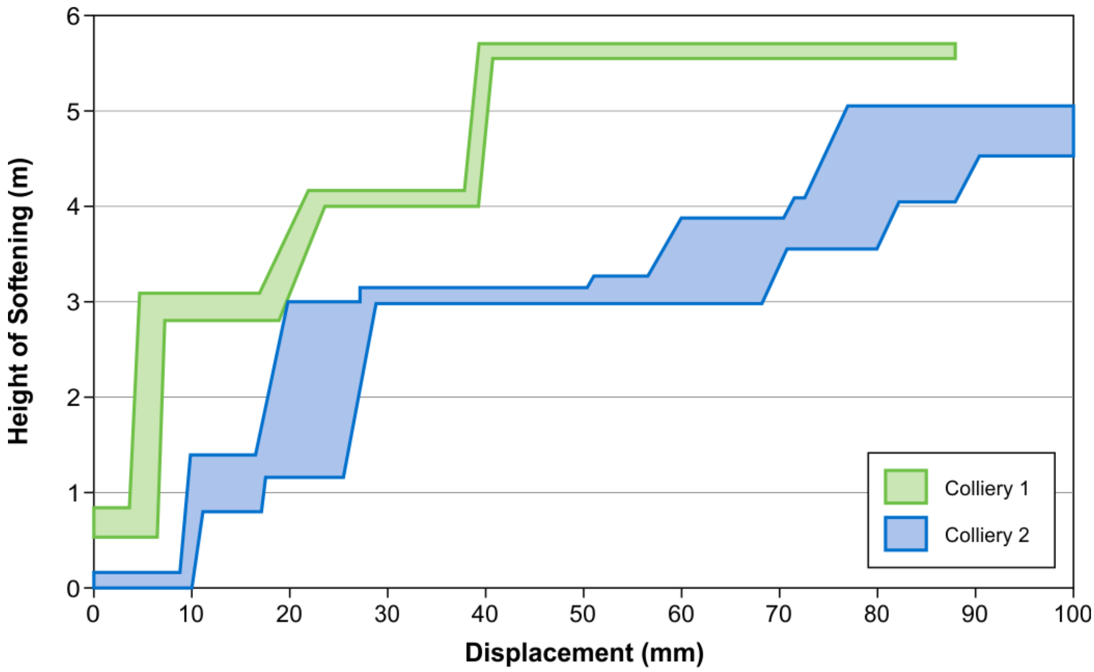

Figure 4: General relationship between roof displacement and height of softening (SCT Training Manual).

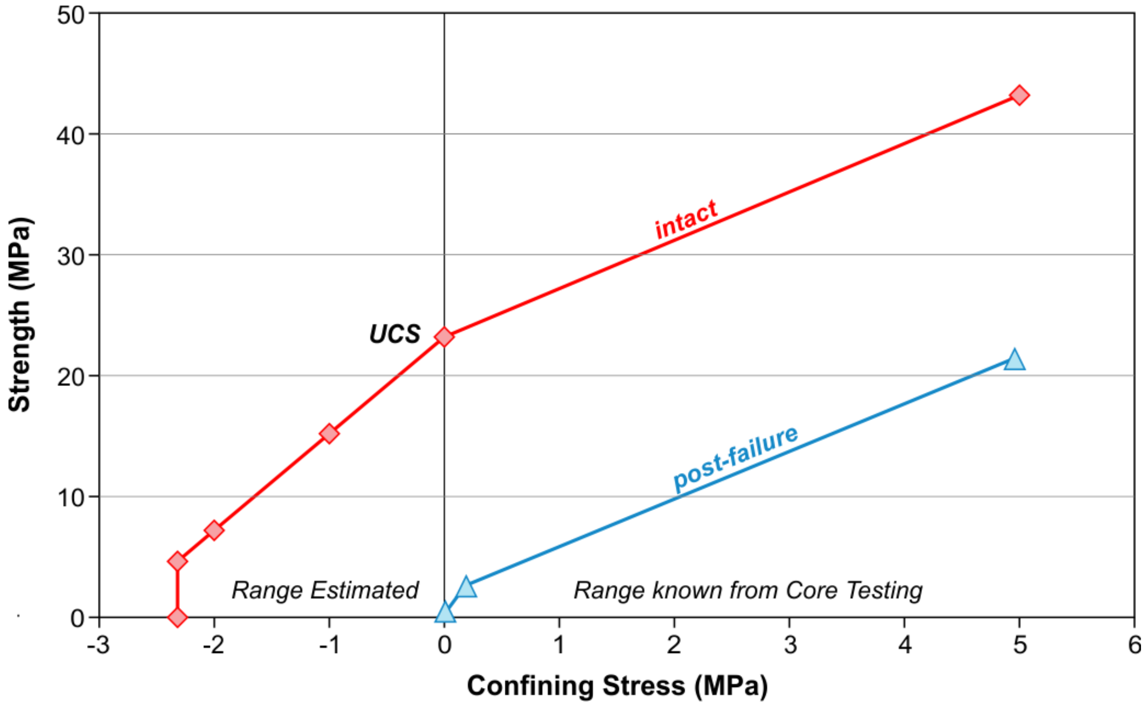

Figure 5: Generalised strength characteristics for rock units (SCT Training Manual).

Geological and geomechanical characterisation of Bulli seam was used for the numerical simulations presented in this paper. Variation of the compressive strength (UCS) of roof and floor strata is presented in Figure 6. These figures show that the UCS of roof and floor strata varies between 10 - 80 MPa and 22 – 60 MPa respectively. Coal seam thickness is 3 m and simulated roadway has 5 m width and 3 m height. Rock support elements include eight roof bolts with 2.1 m length and two rib bolts with 1.2 m length. Depth of simulated roadway is 500.

Table 2: Numbers which used to present various failure modes

Code	Failure Mode	Code	Failure Mode
0	No Failure	7	Tension fracture reactivation in tension
1, 2	Shear fracture reactivation in shear	8	Tension failure of bedding and reactivation in tension
3	Bedding shear and reactivation	9	Shear failure in intact rock
4	Tension Failure or reactivation in shear		
5, 6	Tension reactivation of shear fractures		

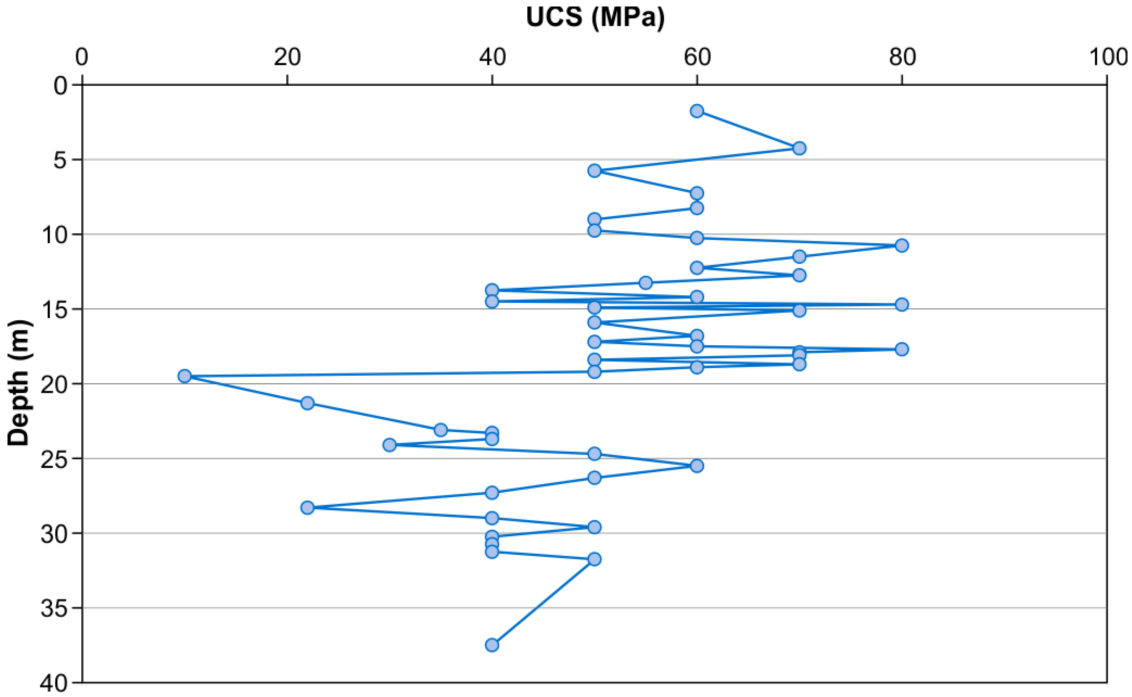

Figure 6: UCS profile through the 3D modelling boundary.

A medium-bedded stratum (based on Table 1) was assumed for the first 3 m of the roof and the floor. The stratum becomes thick-bedded for the rest of the model. In addition to this, two stress orientation scenarios of; 1) a maximum horizontal stress perpendicular to the roadway axis and, 2) a 45 degree between maximum horizontal stress and the roadway axis were modelled.

The results of 3D modelling in the form of failure modes and the extension for two stress orientation scenarios are shown in Figures 7 and 8. It can be seen that the bedding shear failure and re-activation in shear are the failure modes, which control the extension of the failure zone for both stress orientation scenarios. The height of failed zone is approximately 5.3 m and 4.2 m for perpendicular stress and 45 degree stress respectively.

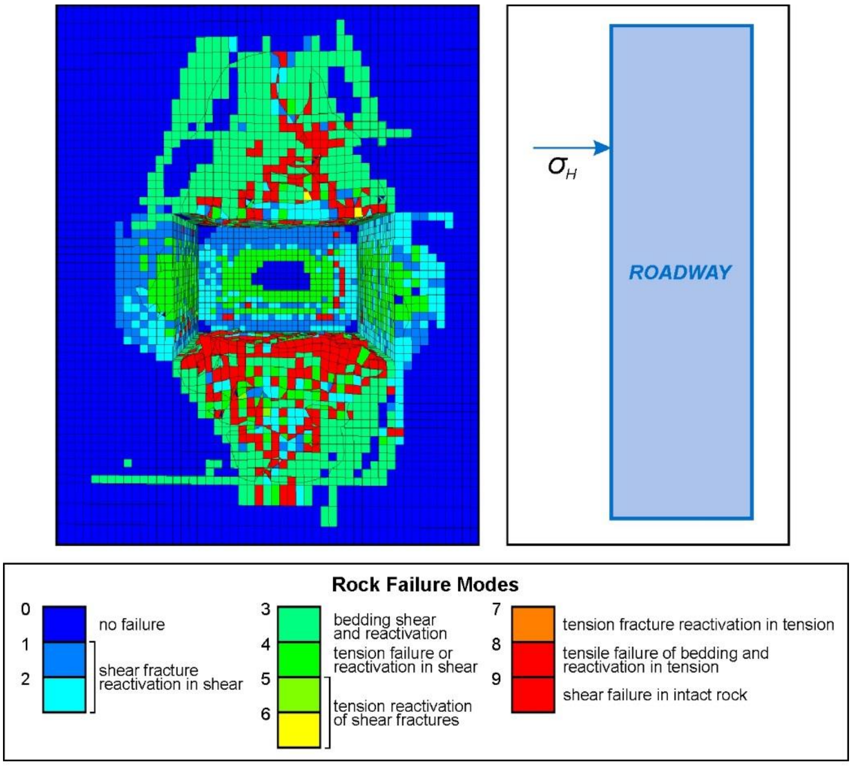

Figure 7: Failure modes and extension for model having bedding planes – stress perpendicular.

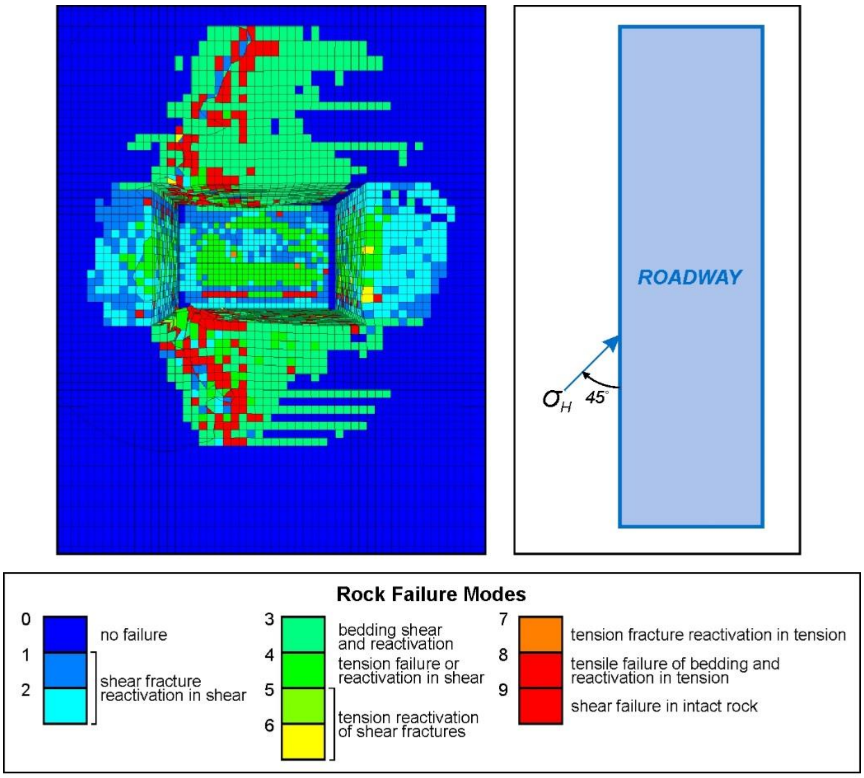

Figure 8: Failure modes and extension for model having bedding planes – stress 45 degree.

From Figure 8, the shear failure through the rock in the roof and floor strata is skewed toward left rib due to the stress orientation impact. The 3D modelling correctly simulated the guttering failure mechanism induced by stress concentration at the left corner of the roof and the floor.

To assess the impact of the bedding planes and laminations on the extension of the softening zone, above modelling were repeated without having bedding planes impact. In this regard, the tensile and shear strength of the bedding planes were increased to eliminate the potential for tensile and shear failure along the bedding planes. This condition can represent a massive unit in roof and floor of the roadway. The failure modes and the extension of the failure zones for two stress orientation scenarios are presented in Figure 9 and 10.

By eliminating the potential for bedding planes failure, the stress redistribution causes shear and tensile failure through the rocks. The extension of the failure zone for both stress orientation scenarios were reduced to 2 m. This height of softening zone is approximately 38% and 48% of the height of softening zones for the models including the bedding planes.

The comparison of the failure modes in Figure 8 with Figure 10 reveals another major impact of the bedding planes to the behaviour of the roadways. The following failure pathways to explain the failure mechanism of roadways within the stratified and laminated rocks correctly obtained from this 3D numerical modelling include (Figure 11):

1. Stress concentration at the left corners of the roadway face breaking bedding planes close to the roof and the floor. This stress concentration also causes shear failure through the rock units.
2. By advancing of the face, the confinement provided by the face rocks decreases. Then the combination of rock shear failure and separation of the bedding planes pushes the stress concentration into the overlaying units.
3. Now, the stress concentration within the overlaying units causes shear failure through the rock and bedding planes. This pushes the stress further toward the roof.
4. This process is repeated until the confined strength of the rock and bedding planes exceeds the concentrated stress and the failure process is stopped.

Above failure pathway can explains the mechanism for the visible guttering formed in roadways. This mechanism shows that the following conditions are required to form the guttering:

1. The elevated stress exceeding the confined strength of the rocks, bedding planes and laminations.
2. The angle between roadway axis and maximum horizontal stress is as low as 10^o and as high as 80^o.
3. There are bedding planes or laminated rocks in the roof to interact with the shear failure of the rocks.

When a massive unit exists in the roof or floor, the shear failure of rock cannot be skewed toward the roadway ribs. The introduced 3D numerical modelling has the capability to simulate all this failure pathways with higher reliability.

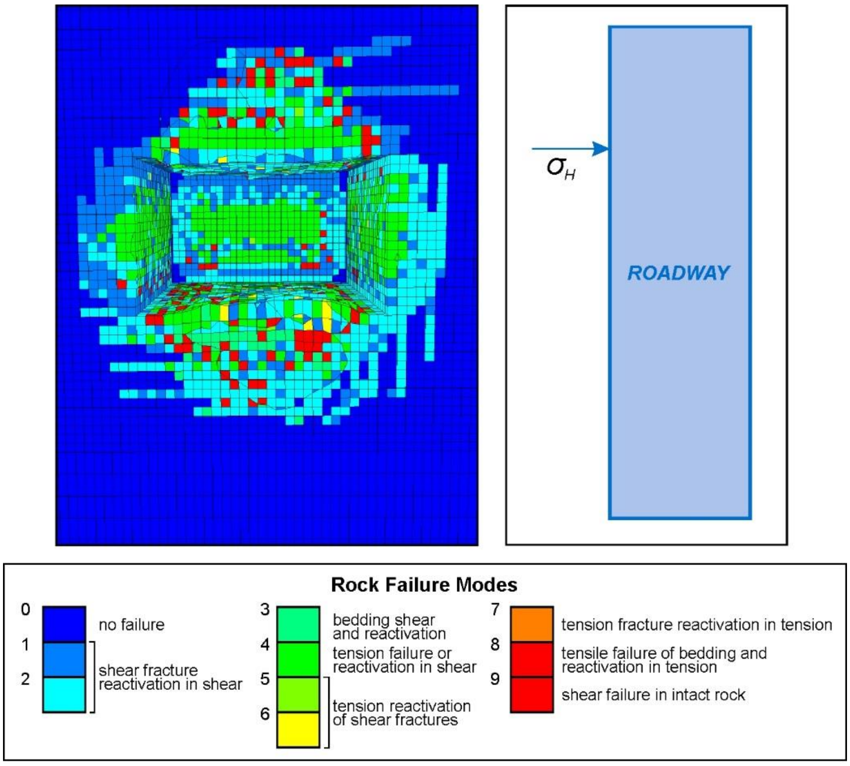

Figure 9: Failure modes and extension for model having no bedding planes – stress perpendicular.

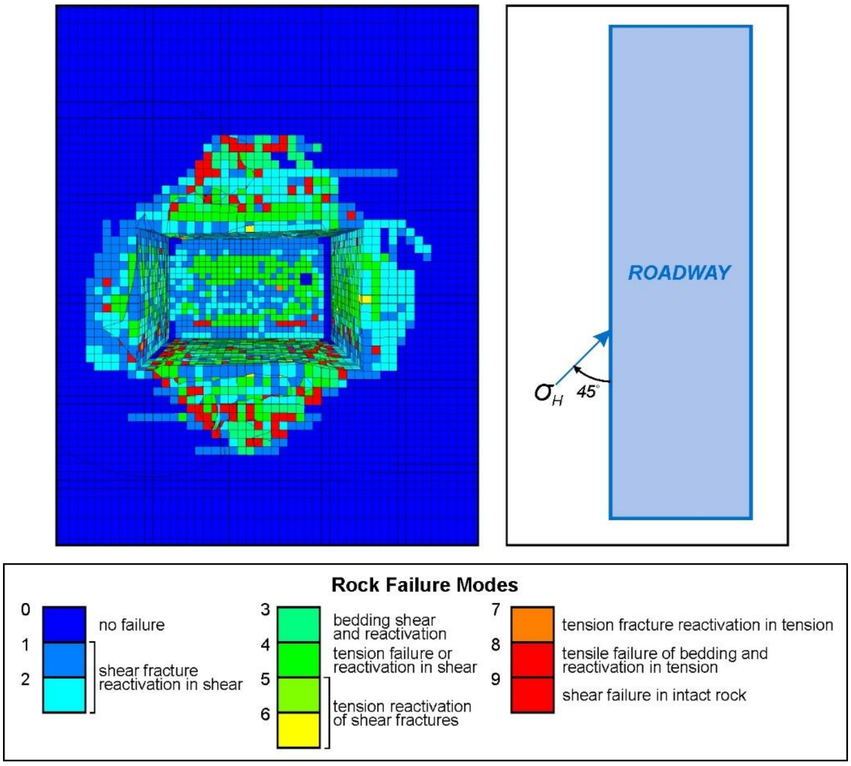

Figure 10: Failure modes and extension for model having no bedding planes – stress 45 degree.

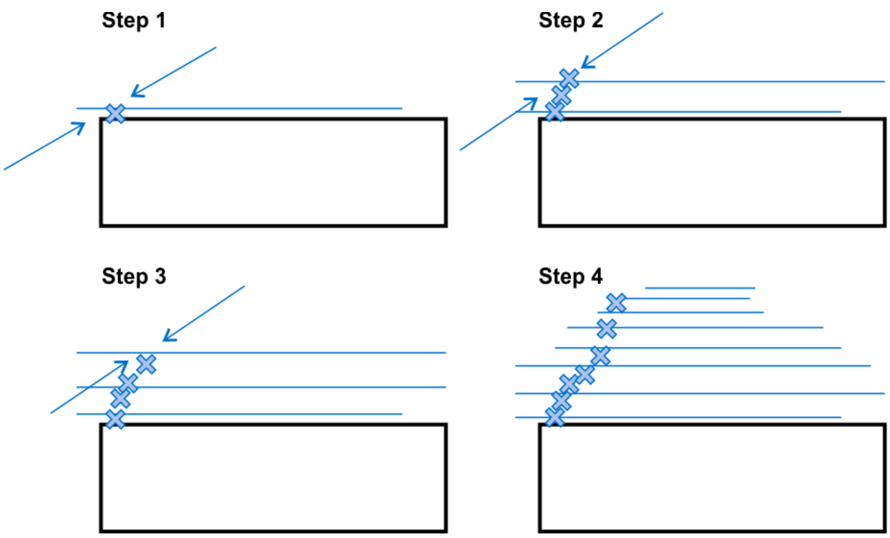

Figure 11: Failure pathway for forming of guttering in stratified and laminated rocks.

CONCLUSION

The impact of the bedding planes and laminations on the failure mechanism and extension of the softening zone around the roadways were studied by 3D numerical modelling. The results of this study show that bedding planes control both the extension of the failure zone and the overall behaviour of the roadways. Bedding planes or laminated rocks in roof increases the height of softening zone in the roof. It also increases the extension of the failure in the floor and raises the potential of floor heave. For cases with maximum horizontal stress having an angle 10-80 degree with the roadway axis, bedding planes skewed the shear failure of the rocks toward the corresponding rib. These conditions facilitate guttering formation in the roof. This study shows that the introduced 3D numerical modelling has the capability to simulate the impact of the bedding planes and laminated rock with high reliability. It provides a powerful tool for stability analysis and roadway reinforcement design.

REFERENCES

Campbell, Ch, 1967. Lamina, laminaset, bed and bedset. Sedimentology, Vol. 8.
Gale, W, 1998. Experience in computer simulation of caving, rock fracture and fluid flow in longwall panels in *Proceedings of the International Conference on Geomechanics/Ground Control Mining and Underground Construction, Wollongong, Australia,* pp: 997-1007.
Itasca Consulting Group Inc. 2013. FLAC3D user guide.
Jaeger, J C and Cook, N G W, 1979. Fundamentals of rock mechanics. Chapman and Hall.
SCT Operations Pty Ltd, 1995. Internal report.
SCT Operations Pty Ltd, 2000. Training manual on coal mine rock mechanics properties.